ICAS 2021 SHANGHAI
International Council of the Aeronautical Sciences
32nd Congress of the International Council of the Aeronautical Sciences
September 6-10, 2021
Pudong Shangri-La, Shanghai, China

AERODYNAMIC DESIGN OF A HIGH-LIFT SYSTEM WITH FLEXIBLE DROOP-NOSE FOR A LONG HAUL BUSINESS JET CONFIGURATION

Min ZHONG[1], Jun HUA[1], Xiasheng SUN[1], Sui ZHENG[1], Ganglin WANG[1], Guoxin ZHANG[1], Hao WANG[1], Yan LI[1], Xiaofei Li[1], Junqiang BAI[2]

[1]Chinese Aeronautical Establishment (CAE), #2 Anwai Beiyuan, 100012, Beijing, China
[2]Northwestern Polytechnical University (NPU), Youyi xilu, 710072, Xi'an, China

Abstract

The flexible droop-nose leading edge is studied and integrated into the aerodynamic design of the high-lift system for the Chinese Aeronautical Establishment - Aerodynamics Validation Model (CAE-AVM) representing a transonic long haul business jet, through numerical and experimental investigations. The high-lift system design techniques and numerical tools have been proven efficient. The innovative configuration of CAE-AVM-HL (High-lift) featuring an inboard flexible droop-nose and outboard slat for the leading edge, a single slot Fowler flap at the trailing edge, provides good balance of the complexity and maximum lift coefficient. A 1:5.6 scale wind tunnel model has been made and tested in the 8x6 meter test section of DNW-LLF, the aerodynamic performance of CAE-AVM-HL with maximum lift coefficient 2.56 and stall angle of attack 19° satisfies design target. The correlation between CFD and experimental results has been validated. The effectiveness of the small flow control fences to eliminate early flow separation near the adjacent area of droop-nose and slat has been demonstrated.

Keywords: Aerodynamic design, High-lift system, Droop-nose leading edge, Flow separation, CFD-wind tunnel correlation

1. Introduction

High-lift system is essential for the aircraft to take-off and landing effectively and safely, it is usually represented with leading edge slats and trailing edge flaps for civil airplanes with large aspect ratio wings. In order to increase the maximum lift coefficient (C_{Lmax}) and the angle of attack (AOA) before stall, the trailing edge flap system used to become more and more complex, from single slot to two or even three slots like Boeing-737-200 and early 747's. With the help of modern design methods and numerical tools such as Computational Fluid Dynamics (CFD) and optimization approach, the flow over high-lift devices could be analyzed more accurately and slot/deflection optimized reasonably so that the number of trailing edge flap slots could be decreased, driven mechanism simplified and even the acoustic noise reduced, like Boeing-787, 747-8 and most of the Airbus airplanes. With the recent efforts to green aviation, the reduction of acoustic noise of the high-lift system is attracting even more attention, including the leading edge devices. It is well known that the leading edge slat is very efficient in increasing stall angle of attach (AOA_{stall}), but the high speed flow stream through the slot between the slat and main wing could be one of the significant sources of noise, therefore some of the latest models applied non-slotted devices such as the solid droop-nose leading edge in the inboard wings of Airbus A-380 and A-350 [1, 2], while Boeing-787 keeps the inboard leading edge slat gapless in the take-off phase.

With the recent progress in morphing technology in structure, materials and measurements, the variable camber wing research became a hot topic worldwide [3,4]. For the high-lift system, variable camber with smooth wing surface could certainly reduce the acoustic noise. For the leading edge, variable camber or flexible droop-nose could not only decrease the noise level, but also be favorable to modern aerodynamic design requiring continuous leading edge surface such as laminar flow wings.

In this paper the aerodynamic design, flow analysis and wind tunnel test of a high-lift system featuring a creative combination of flexible droop-nose, slat and Fowler flap for a long-haul business jet configuration is introduced, the baseline cruise geometry, the design consideration the high-lift system design, the creation of flow separation control fences, the wind tunnel model fabrication and test, together with the CFD – wind tunnel correlation will be discussed in detail.

2. The Development of the Cruise Configuration

2.1 Design and Experimental Study of CAE-AVM Cruise Configuration

The baseline configuration comes from a conceptual study of a long haul business jet at Chinese Aeronautical Establishment (CAE), the airplane length is 35 meters, wing span 33.5 meters including high speed wing tips, and cruise Mach number (M) is 0.87, as shown in Fig. 1. The cruise configuration was designed and optimized via CAE's in-house numerical tools, and satisfactory aerodynamic efficiency is obtained. In order to collect an accurate wind tunnel database for CFD validation with the same model, the wing was redesigned to increase relative thickness T/C around 1% at M=0.85 to reduce the wing aero-elastic deformation of the wind tunnel test model, and this dual purpose configuration was named CAE-AVM (Aerodynamic Validation model). The high speed wind tunnel test model of CAE-AVM was a 1:22 scale full metal structure with 180 pressure taps over 6 wingspan sections built at the Netherlands Aerospace Center (NLR). The model was tested in the German-Dutch Wind Tunnel (DNW) high speed facility DNW-HST in 2013 with M=0.2 to 0.9, for both the verification of the aerodynamic performance and the validation of CFD software. An innovative test scheme was created to perform the simultaneous measurements of forces/moments, pressure coefficient, wing deformation and boundary layer transition in parallel at each polar, to meet the special needs of CFD validation [5-7].

Figure 1 – CAE long haul business jet configuration

2.2 Application of CAE-AVM as a Common Aerodynamic Research Model

Besides other applications, CAE-AVM cruise configuration was used for international investigation of CFD-wind tunnel correlation, due to the verified aerodynamic performance and well correlated numerical and experimental results. Two configurations were released in 2015 to the participants of the CAE-DNW Workshop on CFD-Wind Tunnel Correlation Study, one was the CAE-AVM cruise configuration and the other was the wind tunnel test geometry CAE-AVM-DZ with deformed wings and the Z sting (Fig. 2). 20 aerospace organizations from 9 countries attended the case studies and major observations were summarized. The Workshop was held in March 2016 in Beijing and it is commonly recognized that for comparison with wind tunnel data for civil airplanes flying at M=0.85 level, model aero-elastic deformation and wind tunnel support sting must be taken into account in the CFD analysis [8-12].

Figure 2 – CAE-AVM (left) and CAE-AVM-DZ (right) used in the Workshop

3. The Development of the High-lift Configuration

3.1 Design Consideration of CAE-AVM High-lift System

Based on the cruise configuration, the high-lift (HL) system design of CAE-AVM was followed from 2015 for the take-off and landing phases and to enlarge the database as well. For business jets, the maximum lift coefficient C_{Lmax} for take-off and landing is usually in the range of 1.6 to 2.3. The design condition of CAE-AVM-HL (High-Lift) configuration was targeted at M=0.2, $C_{Lmax} \geqslant$ 2.3 and stall angle of attack $AOA_{stall} \approx 18^{o}$. Meanwhile CFD estimation at wind tunnel Reynolds number Re=3.0e6 is also necessary.

The solid droop-nose, where the leading edge is drooped down as a solid component around a hinge line of its lower end, could reduce both the mechanical complexity and acoustic noise. Furthermore, it will be in favor of laminar flow wings if the droop-nose leading edge is flexible or with continues variable camber and contour, combined with some morphing structures.

In response of green aviation challenges and at the requirement of structure research for variable camber wings at CAE, the high-lift system development of CAE-AVM would study both solid and flexible droop-nose leading edges, and compare with conventional leading edge slat. For the trailing edge, single slot Fowler flap will be considered for simplified driven mechanism and less noise sources.

3.2 Aerodynamic Design Tools for High-lift System

CAE's in-house CFD software AVICFD-Y [13] is used for the high-lift system flow analysis and design, with commercial code Ansys-CFX for case comparison. AVICFD-Y is a Reynolds Averaged Navier-Stokes (RANS) solver accepting multi-block structured grids. The typical 3D mesh for the full aircraft and high-lift devises is in the size of 80 million nodes, as shown in Fig. 3. The CAE's high-lift system optimization tool is a surrogate model based numerical framework developed and verified in 2013, as shown in Fig. 4.

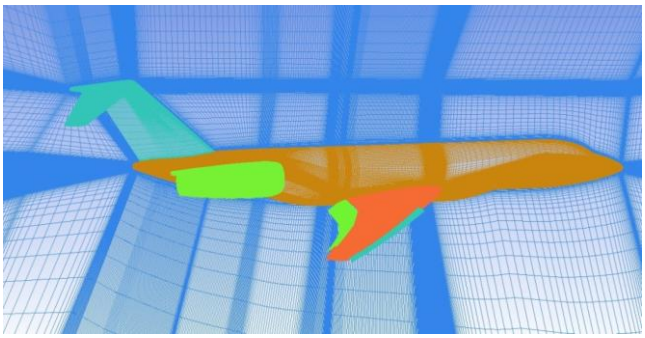

Figure 3 – Typical CFD mesh of CAE-AVM-HL

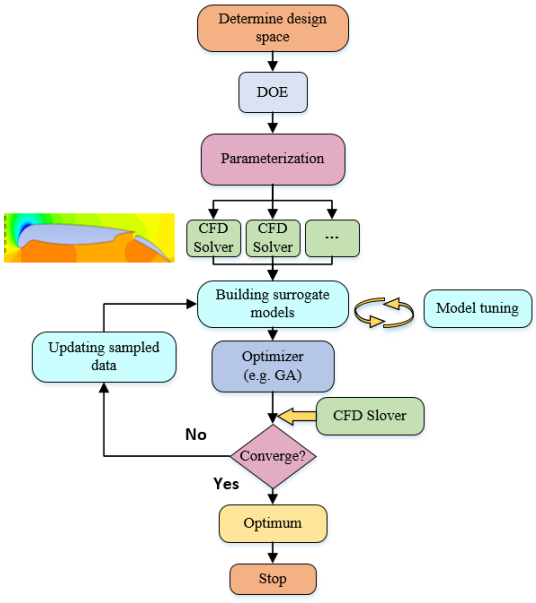

Figure 4 – Flow chart of CAE's high-lift system optimization tool

3.3 Aerodynamic Performance of Leading Edge Droop-nose

The droop-nose designs for both solid deflection and flexible contour were studied. For flexible droop-nose, constant skin length of the morphing leading edge was applied as a constraint, as the stretchable skin materials were still in low technical readiness level (TRL) for the application to the wing leading edge. The major factors to be investigated are deflection angles and leading edge radius, Fig. 5 gives examples of different leading edge radius and their effects in C_{Lmax}. It is found that both solid and flexible droop-nose will have more smooth flows over the leading edge, but the C_{Lmax} and AOA_{stall} are reduced compared to the leading edge slat under similar deflection angles, which is in consistency with other investigations [14].

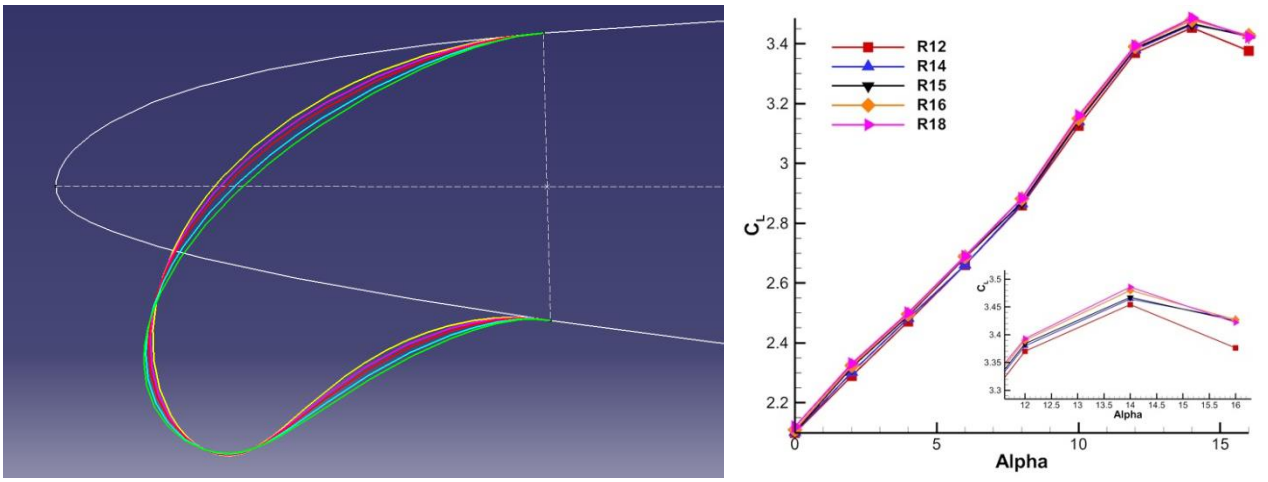

Figure 5 –Different leading edge radius and effects in C_{Lmax}

3.4 Design of the CAE-AVM High-lift Configuration

Three different high-lift systems were designed for the CAE-AVM-HL wing. With a three-segment trailing edge single slot Fowler flap, the leading edge devises included at the beginning a full span slat design; followed by an outboard slat plus a mid-board flexible droop-nose and an inboard solid droop-nose design; and finally an optimized outboard slat plus an inboard flexible droop-nose design was selected as a good balance of the complexity and C_{Lmax}, as shown in Fig. 6.

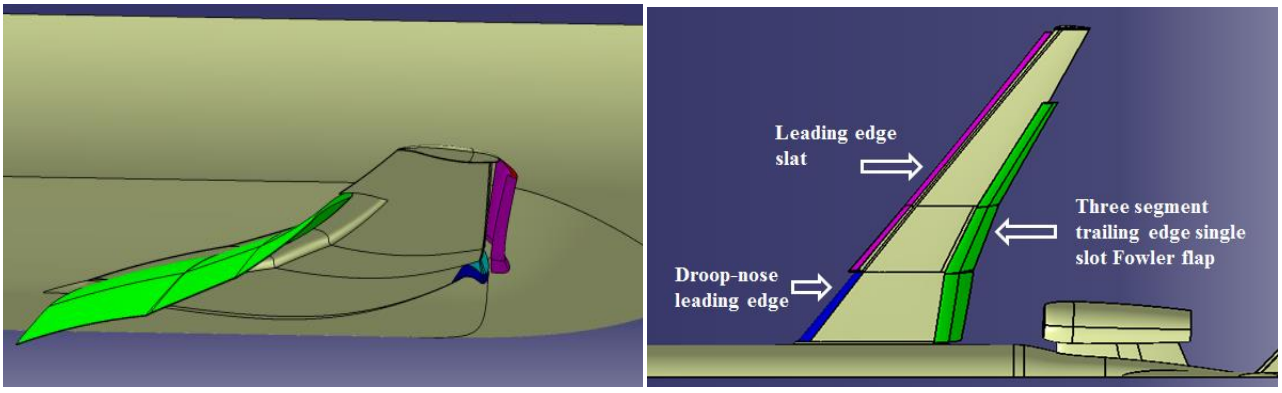

Figure 6 – CAE-AVM-HL with in-board flexible droop-nose

CFD analysis was conducted in detail also at Re=3.0e6 before the wind tunnel test. The estimated C_{Lmax} at this Reynolds number is 2.4 and AOA_{stall} is 18° at the landing flap setting of 31°, slat 22° and droop-nose 30°, which satisfied the design target, as shown in Fig. 7.

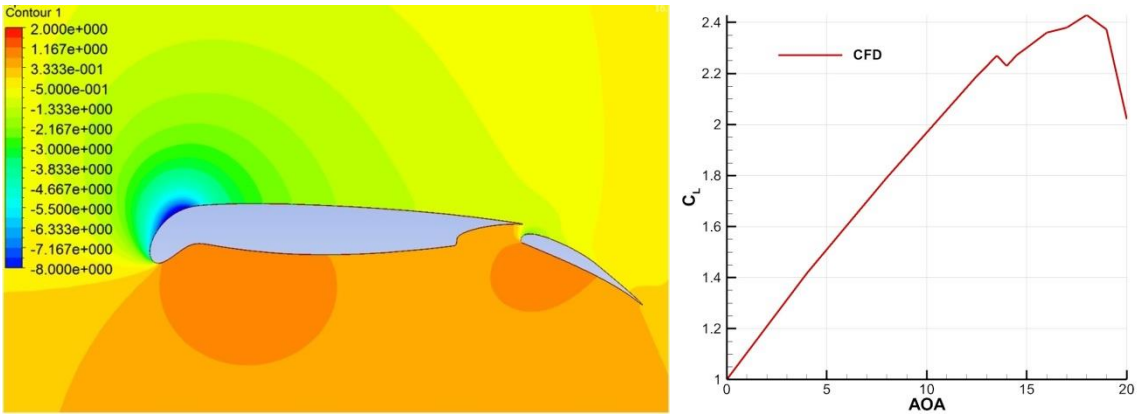

Figure 7 – CFD results of CAE-AVM-HL (left: flow contour; right: C_L-AOA curve)

3.5 Creation of the Flow Separation Control Fences

The span-wise extension of the inboard flexible droop-nose is to 30% semi-span, where the first separation is expected to take place at high AOA to avoid earlier separation at wing tip to affect lateral direction control and the pitching moment, or at wing root to influence the rear fuselage mounted engines. However, CFD analysis indicated an early separation at this 30% span location when AOA=14^o under Re=3.0e6, which caused a small wavy change of the lift curve as shown in Fig. 7. From the detailed analysis of CFD results and flow streamlines, it was found that the local separation is caused by the interference of two flow streams meeting in this adjacent section of droop-nose and slat, one is from the lower side of the droop-nose flowing in the outboard direction, the other is the cross flow in the slot of the slat in the inboard direction, they encounter at the gap between droop-nose and slat, flow towards the upper side of the wing and lead the separation there, as shown in Fig, 8.

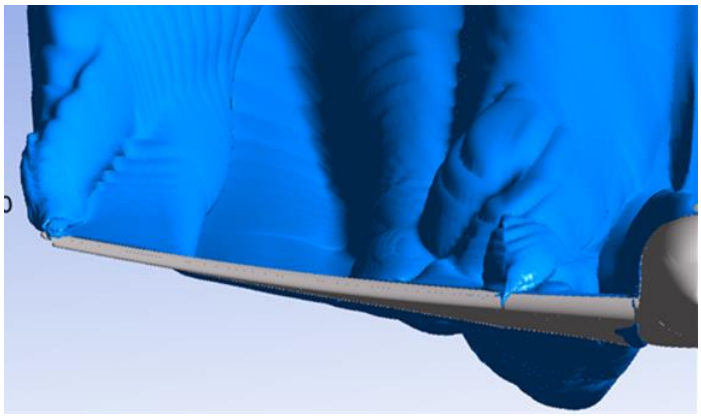

Figure 8 – Separation at droop-nose/slat adjacent section

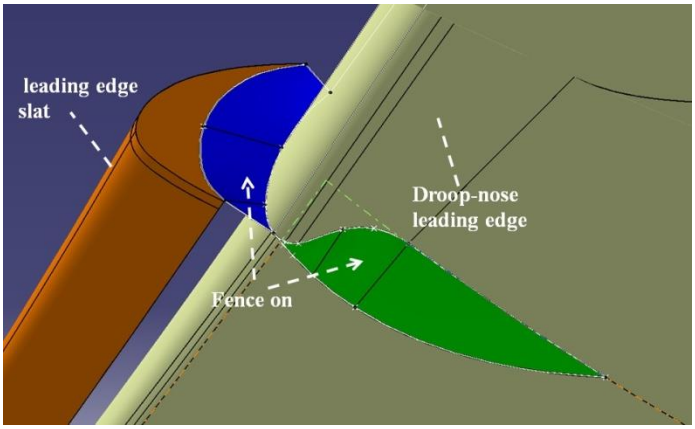

Figure 9 – Separation control fences

In order to postpone this separation to higher AOA, two small flow blocking fences were created and added to control the flow interference, as shown in Fig. 9. The function of the fence-1 (in

purple in Fig. 9) is to block the inboard cross flow stream from the slot of the slat and the main wing, while the fence-2 (in green) is to block the outboard flow stream from the high pressure region of the lower side of droop-nose into the gap and flows to the upper surface of the adjacent area. CFD analysis verified the effectiveness of these simple flow control devices and the local separation was successfully shifted to AOA=17~18 degrees, but still before the separation at wing tip and wing root, meanwhile the C_{Lmax} was increased as well.

4. The Wind Tunnel Test of the High-lift Configuration

4.1 The Wind Tunnel Test Model of CAE-AVM-HL

A 1:5.6 scale model of CAE-AVM-HL was made in Deharde, Germany in 2018. It features a full metal structure and 480 pressure taps in 9 span sections over the droop-nose, slat, main wing and flap, respectively. The principle of brackets design of slat and flap was to have minimum interference to the slot flow, so the number and sizes of brackets would be limited but the strength would be sufficient to keep the stiffness of the slat and flap positions in the wind tunnel test. The aerodynamic loads were provided by CAE from the CFD results and the model structure design was completed in Deharde. The leading edge slat is supported with 8 brackets and the trailing edge flap by 4 brackets only, including a fuselage bracket. The stress analysis indicated that the deformations of the wing and high-lift devices under aerodynamic loads are still within the expected limit when trailing edge flap brackets were reduced from 5 (Fig.10) to 4, and it was verified by the deformation measurements in the followed wind tunnel test. The trailing edge flap brackets were designed with a smart mechanism that the change of flap positions could be done without removing any parts from the wing. The two small separation control fences were combined into a single piece made of carbon fiber composite.

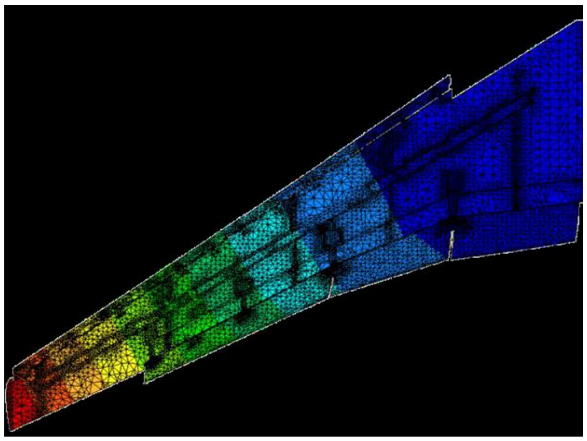

Figure 10 – Stress analysis of the model wing deformation

4.2 The Wind Tunnel Test of CAE-AVM-HL

CAE-AVM-HL model was tested in the DNW large low speed facility DNW-LLF 8x6 meters test section in 2018 (Fig. 11), with detailed simultaneous measurements of forces/moments, pressure distributions and wing/flap deformations, together with flow visualization of PIV, mini-tufts, and colored oil flow techniques. The model was supported with a ventral sting, and both dorsal and dummy stings were applied in the support interference test. The typical test condition was M=0.2, AOA range from -6 to 22 degrees or more, with model chord Reynolds number 3 million. The onsite test data correlated already quite well with the design and CFD analysis, therefore the complete test campaign was smooth and high quality data accumulated.

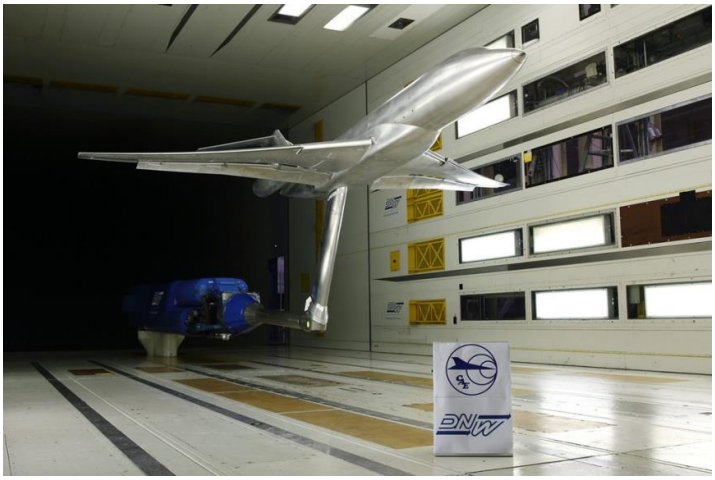

Figure 11 – CAE-AVM-HL model tested in DNW-LLF 8x6 meter test section

5. The Correlation of CFD and Wind Tunnel Test

5.1 Comparison of CFD and Wind Tunnel Date of CAE-AVM-HL

Fig. 12 shows a comparison of CFD and wind tunnel results in C_L-AOA curves without control fence, the coincidence of lift values and the slop of the curves before separation appears quite well, particularly the CFD indicated separation at AOA=14° at the adjacent location of droop-nose and slat, was also represented in the test data, as shown in the enlargement of the plot. Meanwhile, the separation at AOA=14° illustrated by surface limited lines of CFD coincides with the oil flow pattern of the test as shown in Fig. 13.

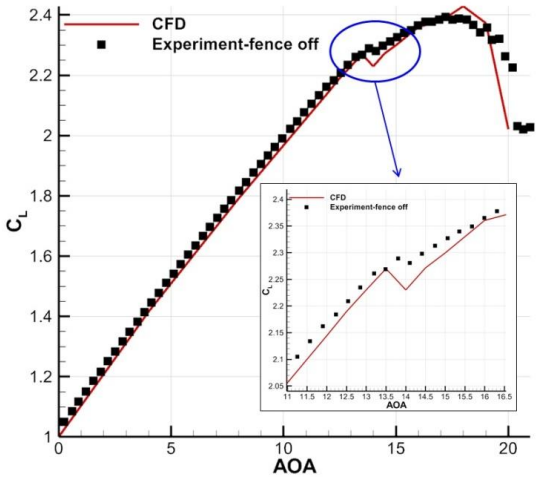

Figure 12 – Comparison of the lift curve of CAE-AVM-HL with fence-off

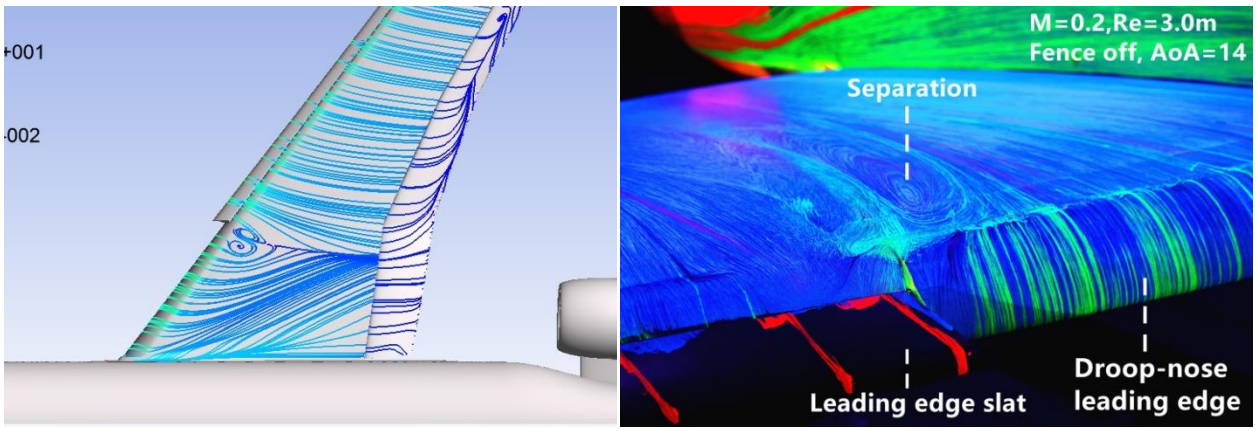

Figure 13 – Comparison of the separation at the adjacent of droop-nose and slat with fence-off

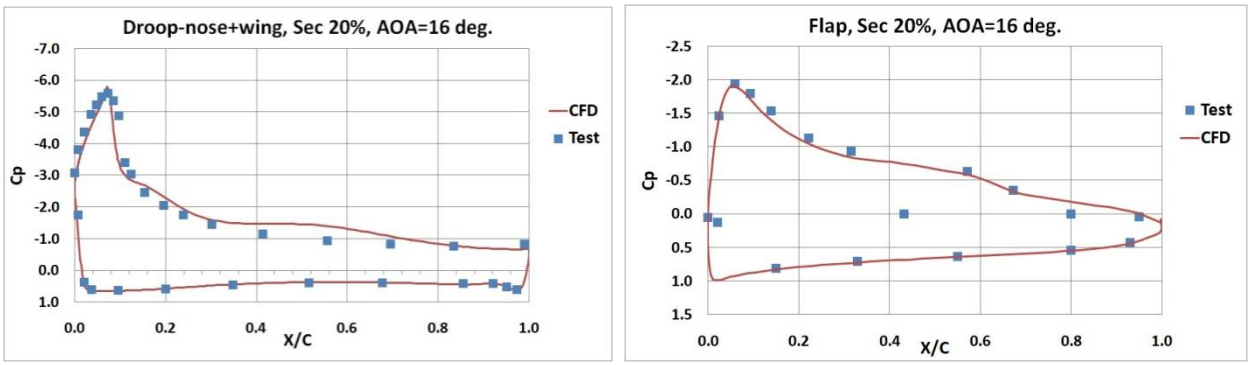

Figure 14 – Cp comparison of droop-nose/main wing (left) and flap (right) with fence-off

Comparison of pressure distributions (Cp) at AOA=16^o are shown in Fig. 14 for the 20% semi-span section where the leading edge is the flexible droop-nose. With fence off, there is already adjacent area separation over the wing upper surface, but the coincidence of Cp in this section is still reasonably good. The slight difference near suction pick at the leading edge may partly due to the possible laminar flow before the transition trip located in 10% chord of the test model, while the CFD is full turbulent. Fig.15 is the Cp comparison at 45% semi-span section at the same AOA, where the leading edge device is slat, the coincidence of CFD and test is much improved.

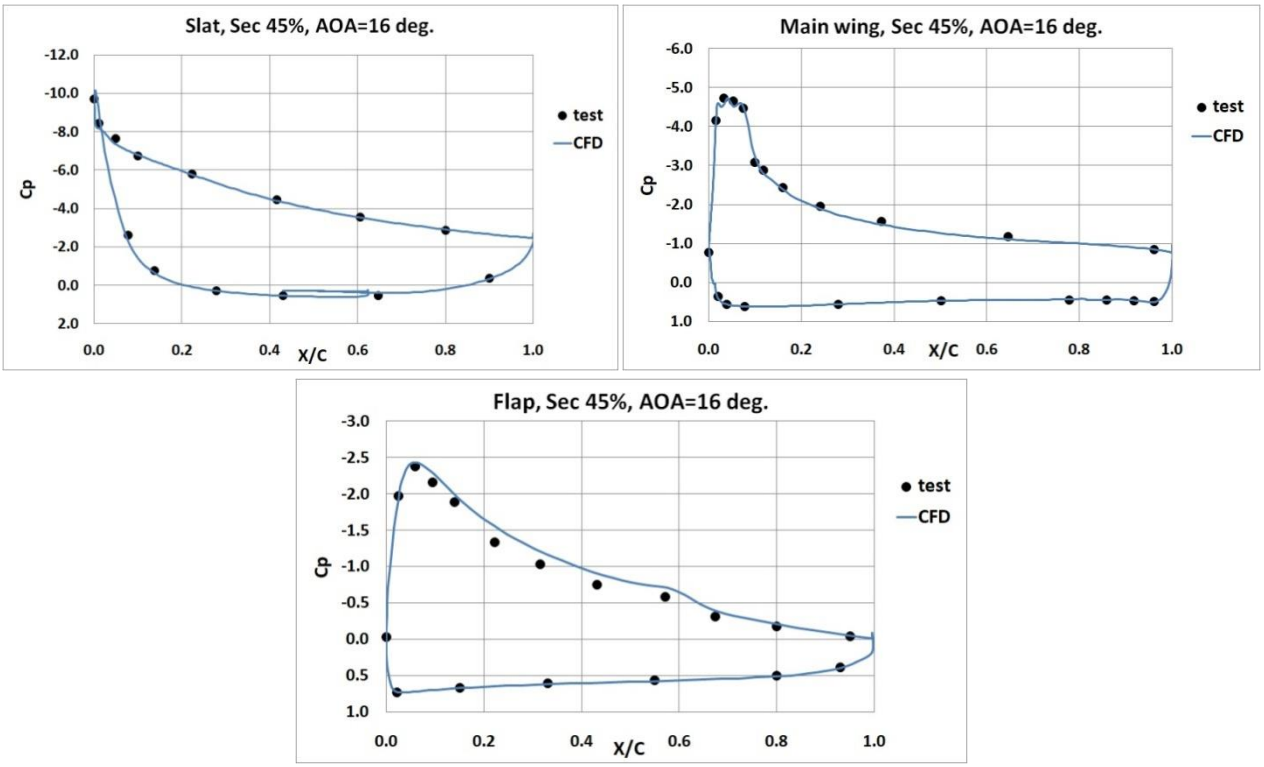

Figure 15 – Cp comparison of slat, main wing and flap with fence-off

5.2 Effectiveness of the Flow Control Fences

Fig. 16 provides a comparison of the lift curves with and without the small flow control fences at the adjacent section of droop-nose and slat. It is clear that, with the control fence on, the early separation at AOA=14^o is postponed and the small wavy change of the lift curve there disappeared. Furthermore, the maximum lift coefficient is increased from 2.4 to 2.56 and the AOA_{stall} shifted by one degree. CFD plot shows that the separation at AOA=14^o has been removed with the control fence on, which again coincides with the oil flow pattern of the test as shown in Fig. 17.

As a result, the effectiveness of the small control fences to eliminate the adjacent area separation and to improve the aerodynamic performance of the high-lift system has been demonstrated.

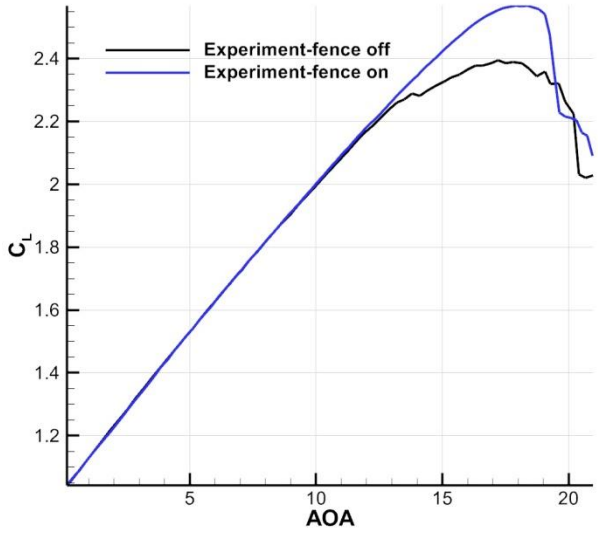

Figure 16 – Comparison of the lift curves with fence-off and fence-on

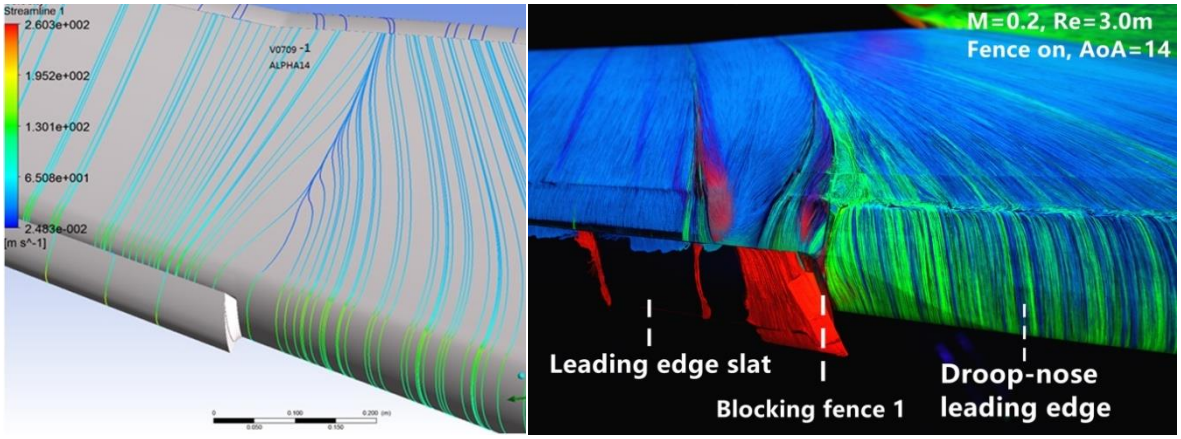

Figure 17 – Comparison of the flow patterns at the adjacent of droop-nose and slat with fence-on

6. The Conclusions

- Flexible droop-nose could improve the leading edge flow, reduce the acoustic noise, and its continues surface has the advantages for laminar flow wings.
- As the aerodynamic characteristics of flexible droop-nose concerning the C_{Lmax} and AOA_{stall} could not match with slat at similar defection angles, the innovative configuration of CAE-AVM-HL with outboard slat plus an inboard flexible droop-nose design for the leading edge, a single slot Fowler flap at the trailing edge, provides good balance of the complexity and C_{Lmax}.
- The design techniques, including the considerations, geometry definition, CFD software and optimization tools applied in CAE-AVM-HL study has been proven effective in high-lift system design.
- The large scale wind tunnel model is accurately made and the wind tunnel test smoothly implemented with high quality data and flow visualization records. It verifies the aerodynamic performance of CAE-AVM-HL configuration with C_{Lmax}=2.56 and AOA_{stall}=19º, well satisfies the design target.
- The correlation between CFD based design and experimental results, including forces/moments, pressure distributions, flow patterns and model deformations has been successfully validated.
- The effectiveness of the small flow control fences for shifting the flow separation near the adjacent of droop-nose and slat has been demonstrated.

Acknowledgment

This investigation was supported by the Innovation Funds of AVIC and other Chinese national

research projects. The authors are grateful to Mr. Henri Vos, Frenk Wubben and Roy Gebbink of DNW, Ms. Silke von Deetzen of Deharde, Mr. Weijia Huang and Ms. Jingnan Zhang of CAE, Ms Li Wang of AVIC, to all the team members of this investigation and to those who have ever contributed to this study.

References

[1] Reckzeh D. Multifunctional wing moveables: design of the A350XWB and the way to future concepts. *29th Congress of ICAS*, St. Petersburg, Russia, ICAS 2014_0133, 2014.

[2] Strüber H. The aerodynamic design of the A350 XWB-900 high lift system. *29th Congress of ICAS*, St. Petersburg, Russia, ICAS 2014_0298, 2014.

[3] Anke Z. Future of aircraft wings: movable leading edge with flexible skin and integrated functions. Press Release, 2015-6-1, 2015.

[4] Li X.F., Zhang M.J, Wang W.J, et al. Research on variable camber wing technology development. *Aeronautical Science & Technology*, Vol. 31, No. 2, pp 12-24, 2020.

[5] Hua J, Zheng S, Zhong M, et al. Design and verification study of an aerodynamic validation model. *7th Asia-Pacific International Symposium on Aerospace Technology,* Cairns, Australia, 2015.

[6] Zhong M, Wang G.L, Hua J. Study of model deformation and sting interference to the aerodynamic estimations of the CAE-AVM model. *30th Congress of ICAS*, Daejeon, South Korea, ICAS-2016-2.7.2, 2016.

[7] Gebbink R, Wang G.L, Zhong M. High-speed wind tunnel test of the CAE-AVM for CFD validation purposes. AIAA-2017-0332, 2017.

[8] Hua J, Zheng S, Zhong M, et al. Recent development of a CFD-wind tunnel correlation study based on CAE-AVM investigation. *Chinese Journal of Aeronautics*, Vol. 31, No. 3, pp 419–428, 2018.

[9] Zhong M, Zheng S, Wang G.L, et al. Correlation analysis of combined and separated effects of wing deformation and support system in the CAE-AVM study. *Chinese Journal of Aeronautics*, Vol. 31, No. 3, pp 429–438, 2018.

[10] Gebbink R, Wang G.L, Zhong M. High-speed wind tunnel test of the CAE aerodynamic validation model. *Chinese Journal of Aeronautics*, Vol. 31, No. 3, pp 439–447, 2018.

[11] Kursakov I, Kazhan E, Gebbink R. Computational study of wing deformation and sting interference effects with the CAE-AVM test case. *Chinese Journal of Aeronautics*, Vol. 31, No. 10, pp 1954-1961, 2018.

[12] Zhong M, Hua J, Sun X.S, et al. Aerodynamic validation model and CFD - wind tunnel correlation. *Aeronautical Science & Technology*, Vol. 31, No. 1, pp 1-16, 2020.

[13] Hua J, “On the Progress of Civil Aviation”, *Von Kamman Institute Lecture Series*, VKI-GRAIN Lectures, 2011.

[14] Burnazzi M, Radespiel R. Design and analysis of a droop nose for Coanda flap applications. *Journal of Aircraft*, Vol. 51, No. 5, pp1567-1579, 2014.

Contact Author Email Address

zhongmin@cae.ac.cn

Copyright Statement